Unified Analytical Synthesis of Cascaded *n*-Tuplets Filters Including Non-Resonant Nodes

Steven Caicedo Mejillones, Matteo Oldoni, Stefano Moscato, Giuseppe Macchiarella, *Fellow, IEEE,* Michele D'Amico, *Senior Member, IEEE,* G. G. Gentili and Goran Biscevic

***Abstract*—This paper presents an analytical method for the synthesis of a low-pass prototype filter constituted by cascaded *n*-tuplets including resonant and non-resonant nodes. The method extends the features of previous published solutions, limited to resonant nodes only or that allow the inclusion of non-resonant nodes but in rigid configurations. The method begins with extracted-pole synthesis, arbitrarily defining the transmission zeros. Then, a filter topology transformation is applied by grouped node blocks to obtain the desired topology, with each *n*-tuplet characterized by the assigned transmission zeros. The procedure overcomes the ad-hoc techniques currently available in the literature. Moreover, the novel filter transformation presented here (from extracted-pole to cross-coupled topology) provides an additional degree of freedom for filter synthesis, which can be further exploited by filter designers. Several examples are presented to validate the novel synthesis procedure.**

***Index Terms*—Cascaded-block synthesis, elliptic filters, filter topology transformation, mixed topology filters, tuplets**

I. Introduction

As wireless communications become more and more pervasive thus fostering 5G evolutions and IoT applications, the requirements on filters in turn aggressively demand extreme selectivity, as usual without yielding to larger size or higher cost. The design of highly selective and compact filters may lead to the introduction of several finite transmission zeros. This conversely often leads to intricate topologies and therefore more complicated implementation and increases the tuning difficulties. Cascaded *n*-tuplets is a well-known topology to overcome these issues. Many works have proposed solutions more or less general to synthesized cascade topologies [1]–[4]. However, the most comprehensive solution is found in [5], where an ingenious procedure is introduced that allows the cascade synthesis of elementary blocks as triplets, quadruplets, quintuplets, sextuplets ($n = 3, 4, 5, 6$) box sections and many others, selected in arbitrary sequence. All the above-mentioned solutions are however limited to only resonant nodes (RN), excluding blocks employing non-resonant nodes (NRN). Although solutions for synthesizing cascaded singlets or doublets ($n = 1, 2$) using NRNs have recently appeared in the literature [6], [7], no analytical synthesis technique is today available for cascaded topologies with arbitrary mixed *n*-tuplets blocks.

This paper attempts to fill this gap by proposing an analytical method for synthesis of cascaded *n*-tuplets of any type (also with NRNs). Furthermore, the novel synthesis method allows including extracted-pole blocks in the synthesized circuit. To the authors' knowledge, this is the first fully analytical method for synthesizing cascaded blocks, including any n-tuplet, non-resonant nodes and extracted pole blocks arbitrarily placed. To this regard, we remark that the solutions available in the literature for mixing extracted-pole and cross-coupled blocks are limited to few rigid configurations [8]–[11].

The proposed method starts with the synthesis of the filter with extracted-pole topology [12], [13]. Then the resulting prototype is suitably partitioned into blocks, after an "extracted pole to cross-coupled" transformation is applied block-by-block to get the desired cascaded *n*-tuplet topology. Two techniques are adopted to carry out the topology transformation: the first is based on the recursive application of the star-to-mesh transformation described in [14], [15], the second one is based solely on the manipulation of the coupling matrix, being easier to implement as a mathematical algorithm. This second method is a generalization to n-order of the technique described in [10] which is focused on third-order blocks. Furthermore, this new topology transformation adds an additional degree of freedom to the synthesis process allowing mixed topologies, which can be thoroughly exploited by filter designers.

The next sections of the paper are organized as follows: Section II provides the description of the synthesis method, while Section III deals with details of the filter topology transformation. Section IV presents several examples to verify the method and finally, Section V summarizes the conclusions.

II. Synthesis Method

A. Extracted-Pole Synthesis

In order to synthesize k cascaded $\{n_1, n_2, ..., n_k\}$-tuplets, the proposed procedure starts with the synthesis of an extracted-pole prototype [12], [13] according to Fig. 1a.

Since the first step in this method is an inline extracted-pole circuit, the first problem that may arise is rounding errors

Manuscript received Oct 15, 2020; revised Jan 15, 2021; accepted Mar 12, 2021. This work was supported by the European Union's Horizon 2020 Research Program 5G STEP FWD under Grant Agreement No. 722429. *(Corresponding author: Steven Caicedo Mejillones.)*

Steven Caicedo Mejillones is with the Dipartimento di Elettronica, Informazione e Bioingegneria, Politecnico Di Milano, 20133 Milan, Italy, and also with the Research and Development Department, SIAE MICROELETTRONICA, 20093 Cologno Monzese, Italy, (e-mail: stevenkleber.caicedo@polimi.it; steven.caicedo@siaemic.com)

Matteo Oldoni, Stefano Moscato and Goran Biscevic are with the Research and Development Department, SIAE MICROELETTRONICA, 20093 Cologno Monzese, Italy (e-mail: matteo.oldoni@siaemic.com; stefano.moscato@siaemic.com; goran.biscevic@siaemic.com).

Giuseppe Macchiarella , Michele. D'Amico and G.G. Gentili are with Dipartimento di Elettronica, Informazione e Bioingegneria, Politecnico di Milano, 20133 Milano (MI), Italy (e-mail: giuseppe.macchiarella@polimi.it; michele.damico@polimi.it; gianguido.gentili@polimi.it).

This is the accepted version of the paper. The published version is available online at https://ieeexplore.ieee.org/document/9419791

Digital Object Identifier 10.1109/TMTT.2021.3073481

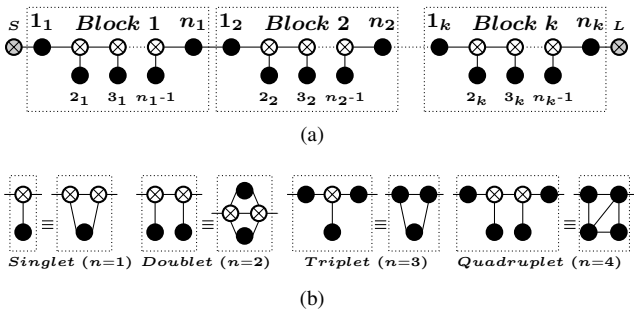

Fig. 1. (a) Extracted-pole Topology. (b) Some equivalences between extracted-pole and n-tuplet blocks. Black circles represent grounded unit capacitance in parallel to frequency-independent susceptances (RN). White crossed circles are frequency-independent susceptances (NRN). Solid lines are admittance inverters. Silver circles are unitary conductance: source (S) or load (L).

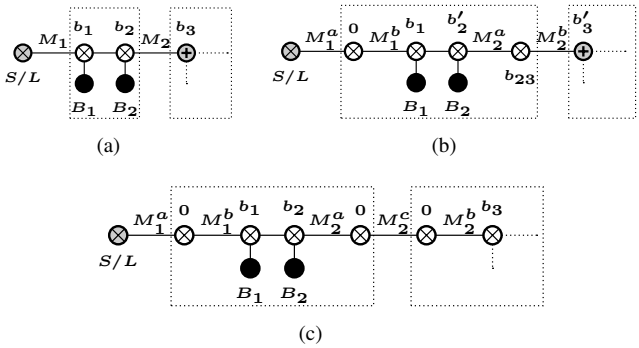

Fig. 2. (a) Equivalent doublet block connected to a S/L and to an adjacent block. (b) Equivalent doublet block after splitting the inverters to a S/L and to the adjacent block into two inverters each. (c) Equivalent doublet block after splitting the inverter to the adjacent block into three inverters. Silver crossed circles are S or L. Silver circle with (+) may be RN or NRN. If the adjacent block is an equivalent singlet or doublet, b_3 is a NRN, otherwise is a RN.

caused by synthesis using section extraction methods [12], which is generally used. However, this can be avoided by using a more accurate procedure, like the one described in [13] and whose synthesis is carried out by matrix rotations. The second issue is that the synthesized extracted-pole circuit is non-physical when complex transmission zeros (TZs) are assigned. However, when the section that performs the complex TZs is transformed into a cross-coupled topology, the circuit becomes physical. The first example of Sect. IV shows this.

Back into the method, a n-tuplet is a circuit of n resonators (RNs) with n-2 TZs, excluding singlets and doublets, in which the number of RNs and TZs are equal. Also, each block of Fig. 1a has n_i RNs and n_i-2 TZs. Then, each block of Fig. 1a is equivalent to a n_i-tuplet; some equivalences are illustrated on Fig.1b. The connection between blocks is through inverters, however, depending on the desired topology, the connection between blocks could be a RN, in which case, the last RN of a block is the first of the next one. If the circuit does not contain the special cases described in Sect. II B, it is ready to be transformed as described in Sect. II C.

B. Inverter-Splitting for Special Cases: singlets and doublets

Blocks equivalent to singlets and doublets must not contain the outer RNs shown in Fig. 1a (compare with Figs. 1b, 2a), since the number of TZ and RNs are equal. In order to obtain the topology required for the transformation in the step of Sect. II-C, dummy NRNs are added by splitting the inverters that connect with adjacent blocks, source or load, as shown in Fig. 2, and following the guidelines below.

1) Block connected to source or load: if a block equivalent to singlet or doublet is connected to a source or load through an inverter (M_1 of Fig. 2a), it is split in a cascade of two inverters. Assigning the first unitary, the other can be found:

$$M_1^a = 1, \;\; M_1^b = M_1. \tag{1}$$

Note in Fig. 2b that the NRN (with 0 susceptance) added between M_1^a and M_1^b is now part of the equivalent singlet or doublet. This step basically amounts to adding a unitary inverter at the input of the filter, affecting only the phase response by a 90° offset in S_{21} and a 180° offset in S_{11}, this phase shift is usually not relevant.

2) Adjacent block is not an equivalent singlet (doublet): it means that b_3 is a RN in Fig. 2a. Therefore, the inverter M_2 can be divided into two inverters and one non-zero NRN as shown in Fig. 2b, therefore [7]:

$$\begin{aligned}(M_2)^{-1} = (M_2^a)^{-1} + (M_2^b)^{-1},\; b_2' = b_2 + M_2 - M_2^a,\\ b_3' = b_3 + M_2 - M_2^b,\; b_{23} = -M_1^a - M_1^b.\end{aligned} \tag{2}$$

Note that either M_2^a or M_2^b can be arbitrarily assigned and that the NRN b_{23} is now part of the equivalent singlet or doublet.

3) Adjacent block is an equivalent singlet (doublet): it means that b_3 is a NRN in Fig. 2a. Depending on the required topology, there are two ways: if it is required that the connection between blocks is through an inverter (Fig 2c), the inverter M_2 can be divided into three inverters and two NRNs with zero susceptance, thus [7]:

$$M_2^c = 1, \;\; M_2 = M_2^a \, M_2^b; \tag{3}$$

if the adjacent singlet (doublet) block is required to share a common NRN, the inverter M_2 can be divided into 2 inverters and 1 non-zero NRN like Fig. 2b; the relations of (2) are still valid. The only difference is that in this case the NRN b_{23} is part of both equivalent singlet (doublet) blocks.

Note that Fig. 2 shows the manipulation of a block which is equivalent to a doublet, but if the nodes b_1 and B_1 are removed and b_2 is directly connected to the source or load (through inverter M_1), we got an equivalent singlet block and all the relations described on this section remains.

C. Circuit Transformation

Each n_i-order extracted-pole block of Fig. 1a is transformed into the cross-coupled topology (n_i-tuplet) by using any of the two methods described in the subsequent section III. The result of this step is shown in Fig. 3. For singlets and doublets blocks the first and last node (1_i, n_i respectively) are NRN, and RN otherwise. Note also that if the chosen topology is the one that connects the n_i-tuplets through a common node, nodes n_i, and 1_{i+1} of adjacent blocks collapse into the same node, and the inverter between them does not exist. To have a mixed topology some blocks can be kept as extracted-poles.

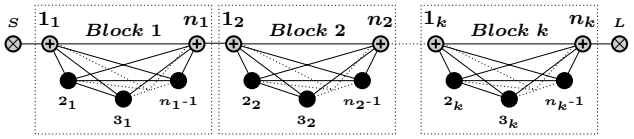

Fig. 3. Cascaded $\{n_1, n_2, ..., n_k\}$-tuplets. Fully cross-coupled circuit on each block. Black circles: RNs. Silver crossed circles are S or L. Silver circle with (+) may be RN or NRN. For doublets and singlets NRN, RN otherwise.

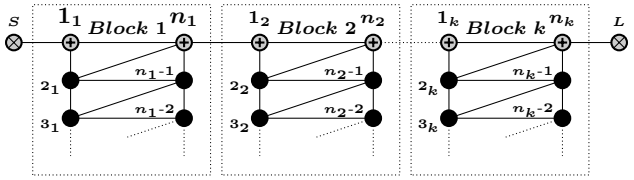

Fig. 4. Cascaded $\{n_1, n_2, ..., n_k\}$-tuplets. Ladder topology on each block. Black circles: RNs. Silver crossed circles are S or L. Silver circles with (+) may be RN or NRN. For doublets and singlets NRN, RN otherwise.

D. Matrix Rotations

The result of the previous step is a fully cross-coupled sub-circuit on each block as shown in Fig. 3, therefore, to obtain a more practical circuit for each block, matrix rotations are required on each block to get the desired cross-coupled topology. The ladder topology (Fig. 4) is the most common topology and the rotation steps to get there from any cross-coupled network are described in [16]. A special case is the doublet topology, whose rotation matrix to get the topology from a fully cross-coupled network is detailed in [7]. No matrix rotation is required for singlets and triplets as they are already fully cross-coupled.

III. Transformation from Extracted-Pole to Cross-Coupled Topology

This section details the transformation of a filter circuit from extracted-pole to cross-coupled topology, providing two methods for this purpose. It starts with the assumption that the extracted-pole circuit described in Fig. 5 (each block of Fig. 1a), is equivalent to an n-tuplet circuit (each block of Fig. 3).

A. Circuit Transformation Method

This method exploits the transformation of the inverters to their π-admittance form [17] (check Fig. 5), and then recursively applying the Star-to-Mesh (S2M) transformation [14], [15] to the circuit.

First, it is necessary to scale the nodes of the circuit in such a way (as shown in Fig. 6) that when the inverters of the already scaled circuit are transformed to their π-admittance form, the total susceptances in all the internal NRNs (i.e. from b_1 to b_{n-2} of Fig. 5) are zero (Fig. 7). Note that the shunt admittances of the π-admittance form of the inverters are absorbed by the NRNs. This leads to solve the system of linear equations (4) to get the scaling values $\overrightarrow{\alpha} = [\alpha_1, \alpha_2, ..., \alpha_k]$.

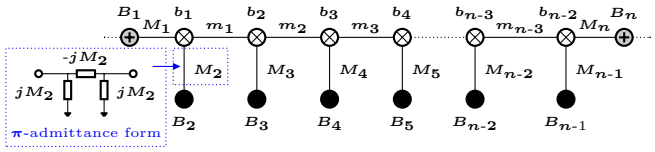

Fig. 5. Extracted Pole Topology. Black circles are RNs. White crossed circles are NRNs. Silver circles with (+) may be RN or NRN. For doublets and singlets NRN, RN otherwise. Solid lines represent admittance inverters.

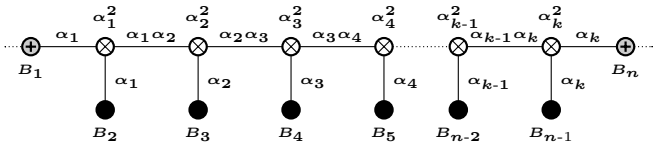

Fig. 6. Manner to scale the extracted-pole circuit. Inverters (solid lines) are scaled by α_i. Susceptances in NRN nodes (crossed circles) by α_i^2.

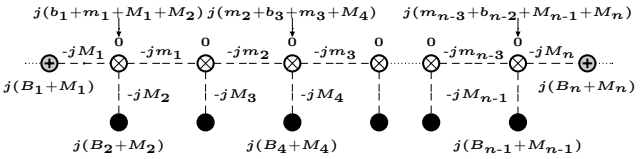

Fig. 7. Extracted pole circuit already scaled with the values from (4), after the conversion of inverters into their π-admittance form. Black circles are RNs. White crossed circles are NRNs, now all with 0 total susceptance toward ground. Silver circles with (+) may be RN or NRN. For doublets and singlets NRN, RN otherwise. Dashed lines are admittances.

$$\overrightarrow{\alpha} = \begin{pmatrix} b_1 & m_1 & 0 & 0 & 0 & 0 & 0 \\ m_1 & b_2 & m_2 & 0 & 0 & 0 & 0 \\ 0 & m_2 & b_3 & m_3 & 0 & 0 & 0 \\ 0 & 0 & m_3 & \ddots & \ddots & 0 & 0 \\ 0 & 0 & 0 & \ddots & b_{n-4} & m_{n-4} & 0 \\ 0 & 0 & 0 & 0 & m_{n-4} & b_{n-3} & m_{n-3} \\ 0 & 0 & 0 & 0 & 0 & m_{n-3} & b_{n-2} \end{pmatrix}^{-1} \begin{pmatrix} -M_1 - M_2 \\ -M_3 \\ -M_4 \\ \vdots \\ -M_{n-3} \\ -M_{n-2} \\ -M_{n-1} - M_n \end{pmatrix} \quad (4)$$

Assuming that the circuit in Fig. 5 has already been scaled with the values derived from (4), then the inverters are converted into their π-admittance form. The resulting circuit is shown in Fig. 7. Note that, as imposed by (4), all the susceptances in the NRNs are zero, it implies that these nodes are now simply connection points, important condition to apply the S2M network transformation.

The circuit is now ready to be transformed. The next step is to perform recursively the S2M network transformation as shown in Fig. 8 by using [14] for every zero NRN :

$$G_{i,j} = \frac{G_i \times G_j}{\sum_{k=1}^{n} G_k}, \quad (5)$$

where $G_{i,j}$ and G_k represents the admittances in the mesh and in the star topology respectively.

The transformation begins in the outer zero NRNs with a 3-node S2M conversion. Then, it continues with 4, 5, ... , p-nodes transformations until reaching the center of the circuit. At this point (Fig. 8d):

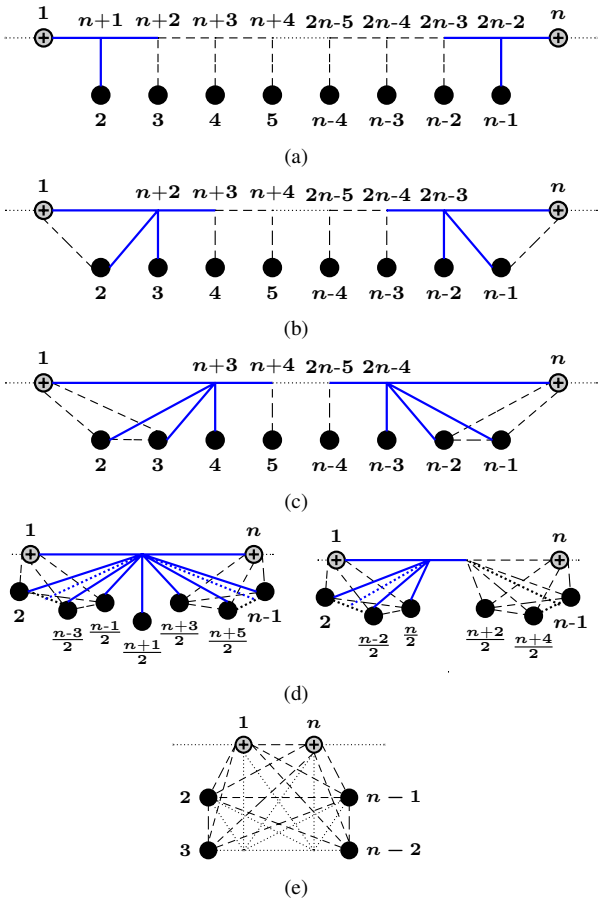

Fig. 8. Topological Transformation. From (a) to (b), star to delta conversions. From (b) to (c), 4-order S2M conversions. (d) Middle of the circuit: left if n is Odd, right if n is even. e) Final fully cross-coupled topology. Dashed lines are admittances. Blue lines are the admittances in star topology ready to be transformed. Black circles are RNs. Circles with (+) are NRN for singlets and doublets, RN otherwise. Nodes from n+1 to $2n$-2 are the zero NRN.

1) if n is odd, there is a node with a shunt admittance in the middle of the circuit, therefore the final step is a n-nodes S2M transformation (Figure 8d-left);
2) if n is even, there is a series admittance in the middle of the circuit, therefore the final steps are: first a $(n+2)/2$ nodes S2M transformation in the left (or right) part of the circuit (Figure 8d-right), the result is similar to Fig. 8d-left but without the central node $(n+1)/2$. Finally, a n-node S2M transformation is required.

The result is the one sketched in Fig. 8e. After the network topology transformation, all the admittances must be re-converted back into inverters [17] following an inverse procedure to the one detailed above between Figs. 5 and 7.

For blocks of extracted-poles to be converted to singlets, doublets, triplets and quadruplets, simple closed form expressions are derived in the next paragraphs, whereas the more general case is described in Sect. III B.

1) Closed-form relation for singlet/triplet: To improve the explanation of the algorithm detailed above, the step-by-step to obtain the relation is presented here. The input circuit is shown in Fig. 9a with coupling matrix detailed in the left part of (7). The first step is to scale node b_1 as shown in Fig. 9b, to ensure that in the next step, its susceptance is 0. α is

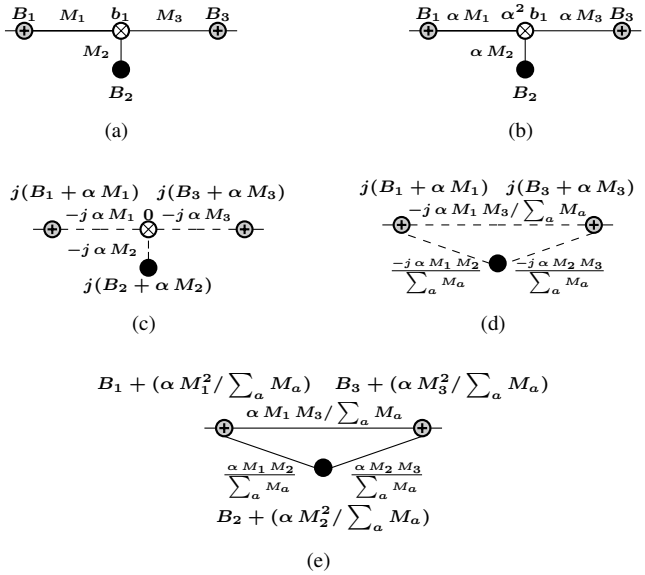

Fig. 9. Extracted pole to singlet/triplet. (a) Extracted Pole. (b) After scaling. (c) After conversion of inverters into the π-admittance form (d) After S2M transformation. (e) Final topology after conversion of admittances into inverters. Solid lines are inverters, dashed lines are admittances. For (a), (b), (d) the labels of the nodes are susceptances, for (c)-(d) are admittances.

calculated with the system (4), here of one dimension:

$$\alpha = -(M_1 + M_2 + M3)/b_1. \tag{6}$$

Then, each inverter is converted into its π-admittance form (check Fig. 5), obtaining the circuit of Fig. 9c. Note that the shunt admittances of the π form are embedded into the nodes, and thanks to the scaling, the susceptance of the NRN is equal to $\alpha^2 b_1 + \alpha(M_1 + M_2 + M_3) = 0$. After this, the star circuit is transformed into delta by using (5), obtaining Fig. 9d. Note that for this case only one transformation was required, however for higher orders the way forward is detailed in the Fig. 8. The final step is to back-transform each admittance that connect two nodes into inverters. The procedure is to complete the π-admittance form on each admittance by adding two shunt admittances (one to each terminal) equal to $j\,\alpha\,M_c\,M_d/\sum_a M_a$, and then convert this π-admittance form into inverter. Note that $-j\,\alpha\,M_c\,M_d/\sum_a M_a$ has to be added to the nodes B_c and B_d in order to not alter the circuit. The final circuit is shown in Fig. 9e. Then, by replacing α in the coupling values of this figure, the output is a cross-coupled circuit represented by the right part of (7).

$$\begin{pmatrix} B_1 & 0 & 0 & M_1 \\ 0 & B_2 & 0 & M_2 \\ 0 & 0 & B_3 & M_3 \\ M_1 & M_2 & M_3 & b_1 \end{pmatrix} \Rightarrow \begin{pmatrix} B_1 & 0 & 0 \\ 0 & B_2 & 0 \\ 0 & 0 & B_3 \end{pmatrix} + \frac{1}{b_1} \begin{pmatrix} -{M_1}^2 & -M_1\,M_2 & -M_1\,M_3 \\ -M_1\,M_2 & -{M_2}^2 & -M_2\,M_3 \\ -M_1\,M_3 & -M_2\,M_3 & -{M_3}^2 \end{pmatrix} \tag{7}$$

Finally, it is important to note that for the triplet case, the nodes B_1, B_2 and B_3 are RNs while b_1 is NRN (which is deleted after the transformation). For the singlet case, instead,

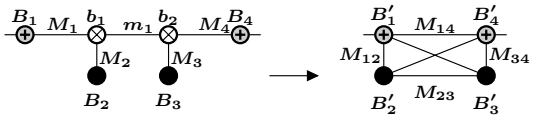

Fig. 10. Extracted-pole to fully cross-coupled equivalence: Doublet or quadruplet. Black circles are RNs. White crossed circles are NRNs. Silver Circles with (+) are NRN for singlets and doublets, RN otherwise. Solid lines represent admittance inverters.

only B_2 is RN; while B_1 and B_3 are the dummy NRNs added after the inverter-splitting procedure described in Sect. II B.

2) Closed-form relation for the doublet/quadruplet: it is represented by Fig. 10 and (8). For the quadruplet case, from B_1 to B_4 are RNs; while b_1, b_2 are NRNs (which are removed by the transformation). For the doublet case, just B_2 and B_3 are RNs; while B_1 and B_4 are the dummy NRNs added after the inverter-splitting procedure described in Sect. II B.

$$\begin{pmatrix} B_1 & 0 & 0 & 0 & M_1 & 0 \\ 0 & B_2 & 0 & 0 & M_2 & 0 \\ 0 & 0 & B_3 & 0 & 0 & M_3 \\ 0 & 0 & 0 & B_4 & 0 & M_4 \\ M_1 & M_2 & 0 & 0 & b_1 & m_1 \\ 0 & 0 & M_3 & M_4 & m_1 & b_2 \end{pmatrix} \Rightarrow \begin{pmatrix} B_1 & 0 & 0 & 0 \\ 0 & B_2 & 0 & 0 \\ 0 & 0 & B_3 & 0 \\ 0 & 0 & 0 & B_4 \end{pmatrix} + \frac{\begin{pmatrix} -b_2\,{M_1}^2 & -b_2\,M_1\,M_2 & M_1\,M_3\,m_1 & M_1\,M_4\,m_1 \\ -b_2\,M_1\,M_2 & -b_2\,{M_2}^2 & M_2\,M_3\,m_1 & M_2\,M_4\,m_1 \\ M_1\,M_3\,m_1 & M_2\,M_3\,m_1 & -b_1\,{M_3}^2 & -b_1\,M_3\,M_4 \\ M_1\,M_4\,m_1 & M_2\,M_4\,m_1 & -b_1\,M_3\,M_4 & -b_1\,{M_4}^2 \end{pmatrix}}{b_1\,b_2 - {m_1}^2} \tag{8}$$

For simplicity, closed-form solutions are not presented for higher orders since expressions become more complex. However, the following section presents a more general approach.

B. Simplified Method Purely Based on Matrix Operations

The coupling matrix M_s of the extracted-pole circuit depicted in Fig. 5 is represented by (10). From (10), the bottom-right sub-matrix $U_{(k\times k)}$ ($k = n-2$) highlighted by the dotted rectangle contains the information about the internal nodes of Fig. 5 (NRNs) and their connections to each other; all these nodes are removed in the transformation procedure. The top-left sub-matrix $X_{(n\times n)}$ highlighted by the dashed rectangle, contains the information about the external nodes of Fig. 5, which are mostly RNs (B_1 and B_n can be RN, NRN, source or load). The top-right sub-matrix $T_{(n\times k)}$ describes the connection between internal and external nodes. Note that because of symmetry, the bottom-left sub-matrix is the transpose of $T_{(n\times k)}$.

By building the nodal admittance matrix for the extracted pole circuit represented by M_s with capacitances C_E in the external nodes, the following can be obtained:

$$j\cdot\left[\begin{pmatrix} X_{(n\times n)} & T_{(n\times k)} \\ T^{\top}_{(k\times n)} & U_{(k\times k)} \end{pmatrix} + \omega\cdot\operatorname{diag}\begin{pmatrix} C_{E(n\times 1)} \\ 0_{(k\times 1)} \end{pmatrix}\right]\cdot \cdot\begin{pmatrix} V_{E(n\times 1)} \\ V_{NRN(k\times 1)} \end{pmatrix} = \begin{pmatrix} I_{E(n\times 1)} \\ 0_{(k\times 1)} \end{pmatrix} \tag{9}$$

$$\begin{pmatrix} \overbrace{\begin{pmatrix} B_1 & 0 & 0 & \cdots & 0 & 0 & 0 \\ 0 & B_2 & 0 & 0 & 0 & 0 & 0 \\ 0 & 0 & B_3 & 0 & 0 & 0 & 0 \\ \vdots & 0 & 0 & \ddots & 0 & 0 & \vdots \\ 0 & 0 & 0 & 0 & B_{n\text{-}2} & 0 & 0 \\ 0 & 0 & 0 & 0 & 0 & B_{n\text{-}1} & 0 \\ 0 & 0 & 0 & \cdots & 0 & 0 & B_n \end{pmatrix}}^{X_{(n\times n)}} & \overbrace{\begin{pmatrix} M_1 & 0 & \cdots & 0 & 0 \\ M_2 & 0 & 0 & 0 & 0 \\ 0 & M_3 & 0 & 0 & 0 \\ : & 0 & \ddots & 0 & : \\ 0 & 0 & 0 & M_{n\text{-}2} & 0 \\ 0 & 0 & 0 & 0 & M_{n\text{-}1} \\ 0 & 0 & \cdots & 0 & M_n \end{pmatrix}}^{T_{(n\times k)}} \\ \underbrace{\begin{pmatrix} M_1 & M_2 & 0 & 0 & 0 & 0 & 0 \\ 0 & 0 & M_3 & 0 & 0 & 0 & 0 \\ : & 0 & 0 & \ddots & 0 & 0 & : \\ 0 & 0 & 0 & 0 & M_{n\text{-}2} & 0 & 0 \\ 0 & 0 & 0 & \cdots & 0 & M_{n\text{-}1} & M_n \end{pmatrix}}_{T^{\top}_{(k\times n)}} & \underbrace{\begin{pmatrix} b_1 & m_1 & 0 & 0 & 0 \\ m_1 & b_2 & m_2 & 0 & 0 \\ 0 & m_2 & \ddots & \ddots & 0 \\ 0 & 0 & \ddots & b_{n\text{-}3} & m_{n\text{-}3} \\ 0 & 0 & 0 & m_{n\text{-}3} & b_{n\text{-}2} \end{pmatrix}}_{U_{(k\times k)}} \end{pmatrix} \tag{10}$$

where C_E represents the vector of n capacitances in the external nodes and V_E and V_{NRN} denote the voltages in external and NRNs respectively. I_E is the total current in the n external nodes. Note that both the capacitance and the total current are zero in the k internal NRNs. Thus, the matrix relation can be decomposed into two blocks:

$$j\cdot\left[X_{(n\times n)} + \omega\cdot\operatorname{diag}\left(C_{E(n\times 1)}\right)\right]\cdot V_{E(n\times 1)} + j\cdot T_{(n\times k)}\cdot V_{NRN(k\times 1)} = I_{E(n\times 1)} \tag{11}$$

$$j\cdot\left[T^{\top}_{(k\times n)}\cdot V_{E(n\times 1)} + U_{(k\times k)}\cdot V_{NRN(k\times 1)}\right] = 0_{(k\times 1)} \tag{12}$$

Then, in order to convert this extracted-pole to cross-coupled topology, the objective is to obtain a relationship involving only the external nodes [10]. To do so, (12) can be solved for V_{NRN}:

$$V_{NRN(k\times 1)} = -\,U^{-1}_{(k\times k)}\cdot T^{\top}_{(k\times n)}\cdot V_{E(n\times 1)} \tag{13}$$

and then (13) is replaced into (11), obtaining:

$$j\cdot\left[X_{(n\times n)} - T_{(n\times k)}\cdot U^{-1}_{(k\times k)}\cdot T^{\top}_{(k\times n)} + \omega\cdot\operatorname{diag}\left(C_E\right)\right]\cdot \cdot V_{E(n\times 1)} = I_{E(n\times 1)} \tag{14}$$

Topologically this means removing the internal NRNs, thus obtaining a cross-coupled topology. Finally, (14) shows that the final cross-coupled coupling matrix M_c is easily obtained by mere matrix operations, and coincides with the third-order formula computed in (7) and [10], also with the four-order detailed in (8), thus extending existing matrix-based techniques to an arbitrary order:

$$M_{c(n\times n)} = X_{(n\times n)} - T_{(n\times k)}\cdot U^{-1}_{(k\times k)}\cdot T^{\top}_{(k\times n)} \tag{15}$$

Note that this method basically consists of implementing (15), and since it is based exclusively on matrices, is easier to implement numerically within an algorithm than that of the previous section, which is based on circuit transformations.

IV. Validation of the Novel Synthesis Method

This section contains five synthesis examples which can be classified into two groups. The first two are purely theoretical, with the purpose of numerically and graphically describing the methodology of the novel synthesis process. The others are practical, which include the physical filter that implements the circuits resulting from the novel synthesis process.

A. Filter prototype with 8 poles and 6 transmission zeros: 2 of them complex for group delay equalization

This example presents the step-by-step synthesis of a filter with: return loss (RL) equals 20 dB, and transmission zeros (TZs) placed at -3, 2, ∞, $-0.1+0.79i$, $-0.1-0.79i$, ∞, 3 and -2 rad/s in the normalized frequency domain.

The first step is the extracted-pole synthesis (Sect. II a), with one possible output is shown in Fig. 11a. Note that the order of the finite TZs can be arbitrarily chosen. However, the positions of TZs at ∞ are driven by the desired output circuit and according to the equivalencies shown in Fig. 1b. We choose to target the outcome shown in Fig. 11d. Furthermore, Fig. 11a highlight with curly brackets the block-by-block equivalences between the extracted-pole circuit and the expected outcome.

Since the expected outcome contains a singlet and a doublet; thus the two inverters highlighted with dashed lines were split (Sect. II b) into two inverters by using Fig. 2b and (2), the output is shown in Fig. 11b. Then, circuit transformations (Sect. II c) were performed by blocks to get the circuit of Fig. 11c. Note that blocks on this figure are fully cross-coupled, finally matrix rotations were performed also by blocks (Sect. II d) in order to get a more practical circuit as shown in Fig. 11d. The scattering parameters and group delay response for all these circuits are shown in Figs. 11 e and f respectively.

In this example it is important to highlight that despite the initial circuit (Fig. 11a) is non-physical and non-passive in the section with the complex conjugated TZs (there are complex numbers and some of them are equivalent to negative resistors); when this section is transformed into a quadruplet (Fig. 11d), a physical, passive and loss-less circuit is obtained. This is an important feature of the novel synthesis method, since it also allows to introduce group delay equalizer transmission zeros in extracted-pole circuits through cross-coupled sections like the circuit shown in Fig. 12a.

Fig. 12 shows three other circuits synthesizable, based on the same initial extracted-pole circuit shown in Fig. 11a. It is also possible to change the position of the TZs in the first step, expanding the number of synthesizable circuits. The filter response of these circuits is still Figs. 11 e-f.

B. Filter prototype with 10 poles and 6 transmission zeros

This example aims to highlight the flexibility of the novel synthesis method, allowing to choose from a wide range of topologies for the same specifications: consider a filter with TZs placed at ∞, 2, -1.5, ∞, ∞, 3, -3, 4, -4, ∞ rad/s and RL of 25 dB. The filter response, according to these specifications, is shown in Fig. 13a and the output of the initial step in Fig. 13b, highlighting equivalences between extracted-pole and n-tuplets blocks. According to these equivalences, the

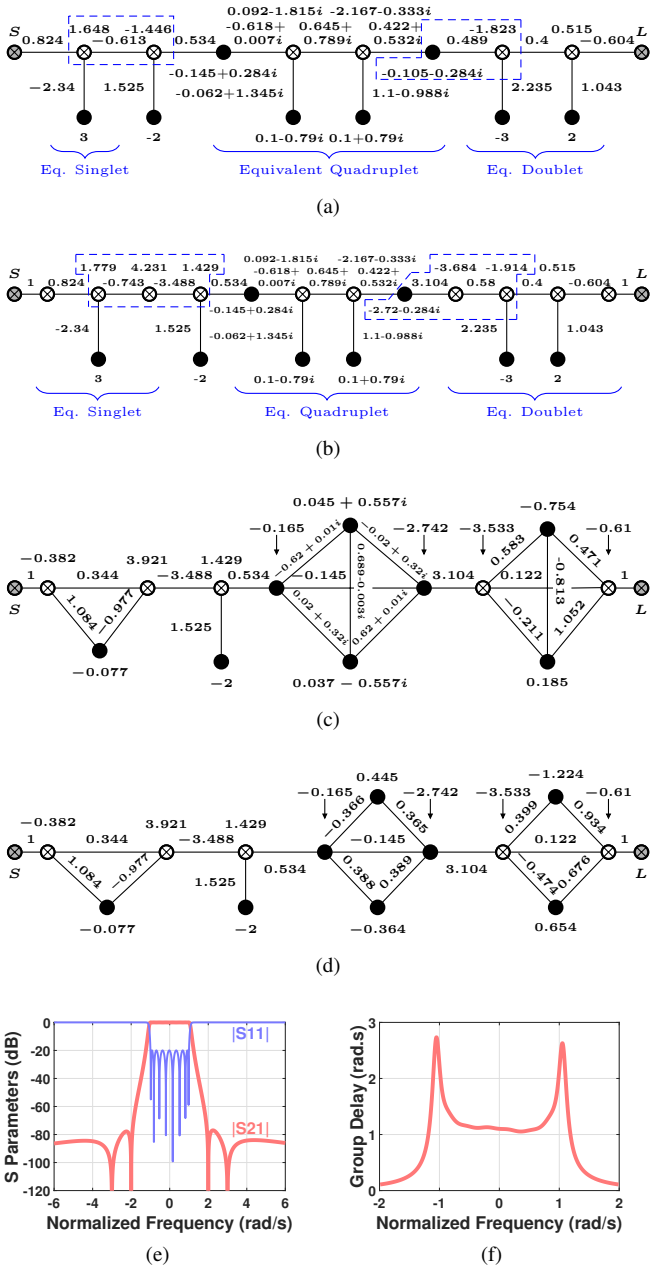

Fig. 11. 8-poles 6-TZ filter. (a) Extracted pole synthesis (Sect. II a). (b) Splitting inverters (Sect. II b). (c) After circuit transformations (Sect. IIc, Sect. III). (d) Cascaded singlet - extracted-pole - quadruplet - doublet. (e) Scattering parameters. (f) Group Delay. Black circles are RNs with unitary capacitance. Silver crossed circles are unitary source or load. White crossed circles are NRNs. Solid lines are admittance inverters.

filter response can be obtained, for instance, via the following cascaded configurations (each described from source to load):

- resonator - doublet - resonator - sextuplet (Fig.13c), to synthesize this circuit, the inverters equal to 0.693 and 0.615 of the extracted-pole circuit in Fig. 13b were split into two inverters each following the guidelines detailed in Sec. II-B, the relations detailed in Fig. 2b and (2) were here. Then, circuit transformations are done on each block (doublet, sextuplet), obtaining the desired topology.
- quadruplet- resonator- doublet- doublet- resonator (Fig. 13d), note that doublets are connected through unitary

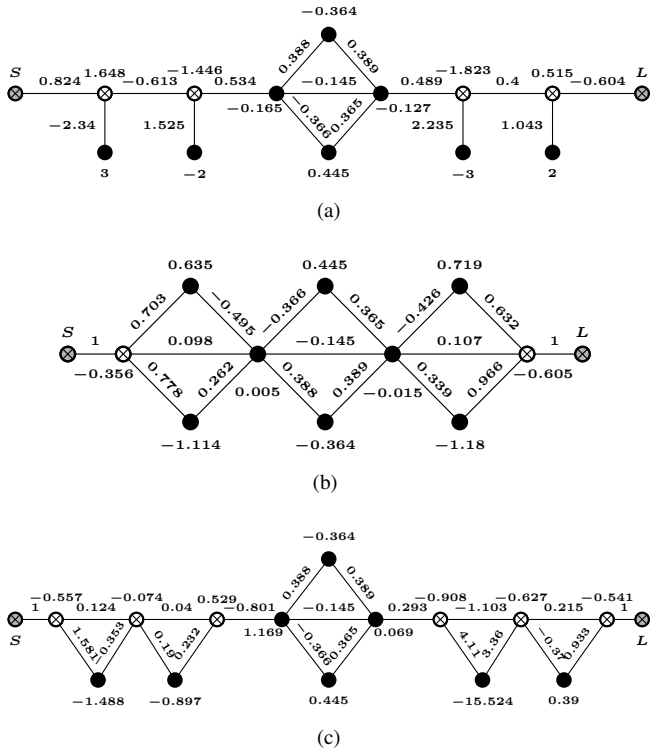

Fig. 12. 8-poles 6-TZ filter. (a) Extracted pole with cross-coupled section performing complex TZs. (b) Cascaded quadruplets. (c) Cascaded singlet - singlet - quadruplet - singlet - singlet. Black circles are RNs. Silver circles are unitary S or L. White circles are NRNs. Solid lines are admittance inverters.

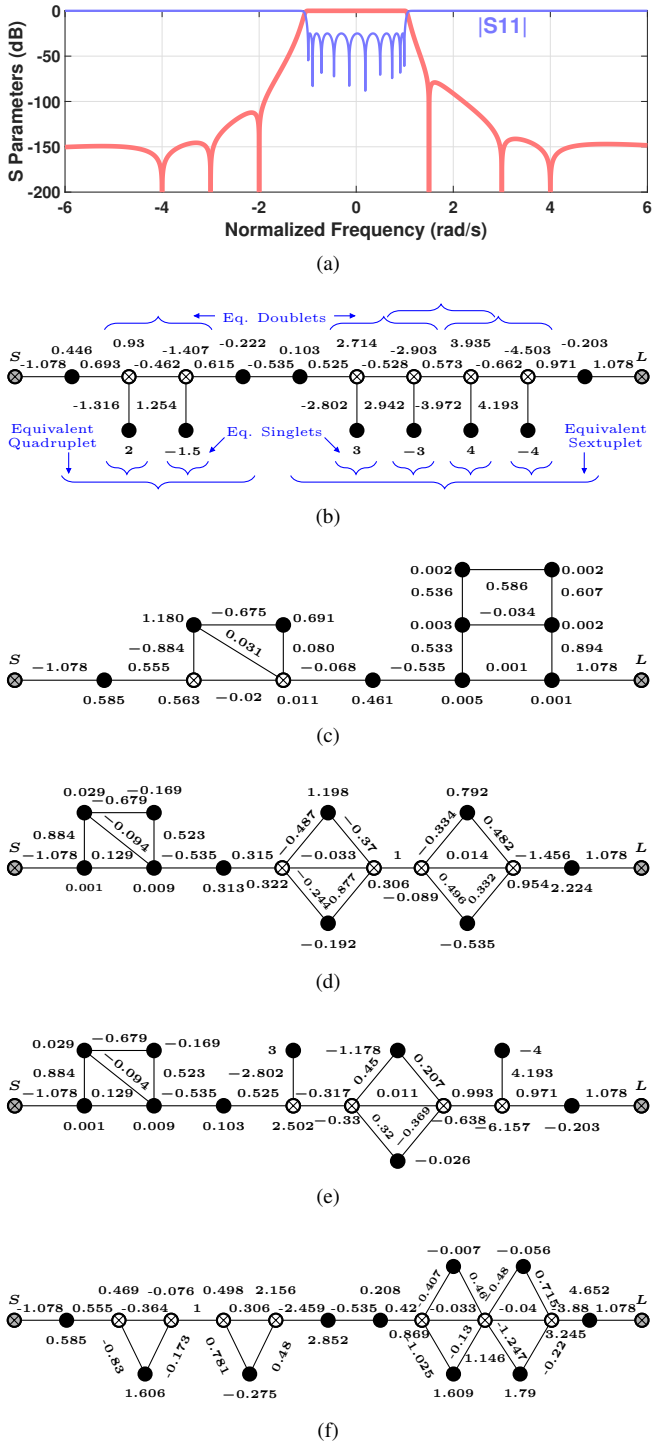

Fig. 13. 10-poles 6-TZ filter. (a) Scattering parameter response. (b) Output of the first step highlighting equivalences between extracted-pole and n-tuplets blocks. From (c) - (f) cascaded configurations of: (c) resonator-doublet-resonator - sextuplet; (d) quadruplet - resonator - doublet - doublet - resonator; (e) quadruplet - resonator - extracted-pole - doublet - extracted-pole - resonator; (f) resonator - singlet - singlet - resonator - resonator - doublet - doublet - resonator.

inverters, it means that before the circuit transformation, the inverter equals to 0.573 in Fig. 13b was split into 3 inverters by using Fig. 2c and (3); inverters equal to 0.525 and 0.971 in Fig. 13b that connect equivalent doublets with the rest of the circuit were split into 2 by using Fig. 2b and (2), also before the circuit transformation;

- quadruplet - resonator - extracted-pole - doublet - extracted-pole - resonator (Fig.13e), inverters equal to -0.528 and -0.662 in Fig. 13b that connect the equivalent doublet with the rest of the circuit was split into 2 inverters, also before the circuit transformation;
- resonator - singlet - singlet - resonator - resonator - doublet - doublet - resonator (Fig.13e), inverters equal to 0.693, 0.615, 0.525 and 0.971 in Fig. 13b that connect equivalent singlet and doublets with the rest of the circuit were split into 2; inverter equals to -0.462 in Fig. 13b was split into 3 in order to get singlets connected through unitary inverters; inverter equals to 0.573 in Fig. 13b was split into 2 in order to get doublets with a common NRN;
- other configurations highlighted in the equivalences of Fig.13b, like quadruplet - sextuplet.

Here is important to emphasize that circuits that contains NRNs can be scaled to get a circuit that fits with specific physical constrains. Also, that by altering the position of the TZs in the first step, other topologies are also synthesizable.

C. Fully canonical filter with 3 poles and 3 transmission zeros

The specifications here considered are: the passband spans from 9.966 to 10.045 GHz, RL of 16 dB and TZs placed at 9.823, 10.17 and 9.8 GHz. The order defined for TZs is the same as in the subsequent circuits. There are many synthesizable circuits for the same specifications as was described before. For this example, two of them are considered. The first is the cascaded singlet-singlet-singlet shown in Fig. 14a.

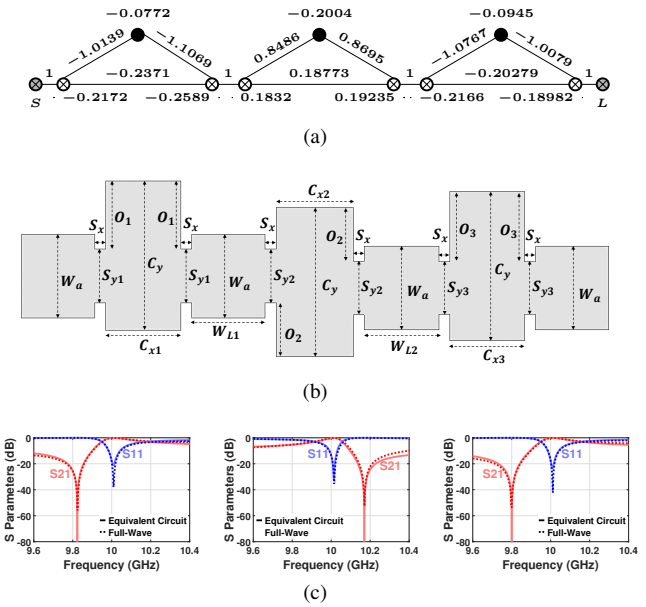

Fig. 14. Cascaded singlet-singlet-singlet. (a) Synthesized circuit, unitary inverters are equivalent to 90° phase shift with unitary impedance. Black circles are RNs denormalized with C=$1/(2\pi\, BW)$, L=$1/(C*(2\,\pi\, F_c)^2)$. BW is bandwidth. Silver crossed circles are unitary source or load. White crossed circles are NRNs. (b) Physical circuit. Each oversized TE cavity is equivalent to the corresponding singlet. A transmission line (WR90) is included at the input and output of each cavity to guarantee equivalences also in phase. WR90 transmission line with 90° of electrical length are the unitary inverters. Dimensions in mm: W_a=22.86, h=10.16, C_y=40.806, C_{x1}=20.484, C_{x2}=21.047, C_{x3}=20.372, S_x=3, S_{y1}=14.699, S_{y2}=14.654, S_{y3}=14.294, O_1=18.6255, S_2=14.723, O_3=19.298, W_{L1}=20.0738, W_{L2}=20.4047. (c) Frequency response of the corresponding singlet (circuit) / cavity (full-wave).

Each singlet implements one corresponding TZ according to the filter specifications. Each one is physically implemented with an oversized cavity with TE_{201} as resonating mode, and the unitary inverters with a quarter wavelength waveguide section [18], WR90 in this case, as shown in Fig. 14b. Each cavity is then optimized to have the response (in magnitude) similar to the equivalent singlet, for the equivalences in phase a transmission line (WR90 in this case) is added at the input and output of each cavity [6]. Fig. 14c shows the scattering parameter response of each singlet (solid lines) compared with the response of the corresponding cavity (dotted lines).

The second circuit considered is cascaded extracted-pole - singlet - extracted-pole as shown in Fig. 15a. Note that this circuit was synthesized and the NRNs scaled in such a way that by converting the inverters 1.0041 and 1.0044 into phase shifters and two shunt susceptances, the NRNs of the extracted-pole blocks are collapsed (equal to 0) by absorbing these susceptances, as shown in Fig. 15b. This circuit was implemented following the same guidelines described before. Thanks to the absence of NRNs in the extracted-pole blocks, they were implemented with a transmission line with a shunt stub as show in Fig. 15c. From left to right Fig. 15d shows the frequency response of the extracted-pole - singlet - extracted-pole with solid lines and of their corresponding physical circuit with dotted lines.

Note that the circuital/physical frequency responses of each block are not as close as in the previous example. This is

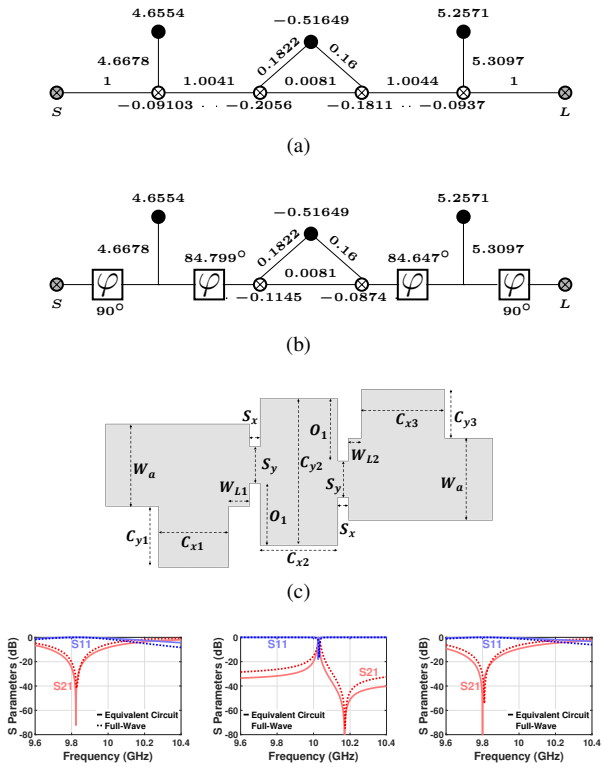

Fig. 15. Cascaded extracted-pole - singlet - extracted-pole. (a) Synthesized circuit. Black circles are denormalized RNs. Silver circles are unitary source or load. White circles are NRNs. (b) Circuit after conversion of inverters that connect blocks into phase shifters with central frequency as reference and unitary impedance. (c) Physical circuit. The oversized TE cavity is the singlet. The extracted-pole blocks are WR90 transmission lines with a stub (there is no NRN in the equivalent extracted-pole circuits of (b)). Dimensions in mm: W_a=22.86, h=10.16, C_{x1}=19.54, C_{y1}=17, C_{x2}=21.622, C_{y2}=40.806, C_{x3}=23.04, C_{y3}=13.59, S_x=2.98, S_y=10.166, O_1=17.304, W_{L1}=5.754, W_{L2}=3.603. (d) Frequency response of each physical block (dotted lines) with the corresponding equivalent circuit (solid lines).

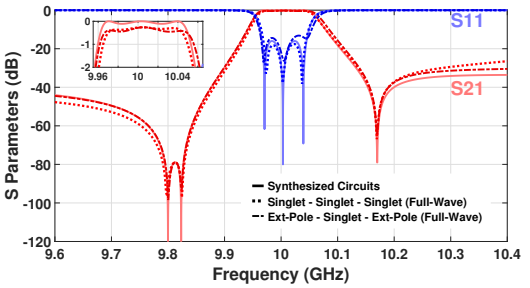

Fig. 16. Scattering parameters of: synthesized circuits of Figs. 14a and 15a-b (solid line), physical circuit of Fig. 14b (dotted line, HFSS simulation), and physical circuit of Fig. 15c (dotted-dashed line, HFSS simulation).

because unlike the previous case, after assembling the entire physical circuit, a fine tuning was required. This is because the stubs are relatively close to the cavity, producing a cross-coupling between them. Also note that under this last topology, a smaller filter length is possible (79.159 mm) compared to cascaded singlets (120.381 mm). Dimensions are without considering the input and output waveguides for both cases.

Finally, Fig. 16 shows the scattering parameter response of the entire circuit: in solid lines the response of the circuital

model, in dotted lines of the physical filter of Fig. 14b, and in dotted-dashed line the response of Fig. 15c. Full wave simulations were performed with Ansys Electronics Desktop, physical dimensions are written in the corresponding captions, and the material used for the simulations was aluminum.

As a remark, singlets can also be implemented with an oversized TM cavity (TM_{110} as resonating mode) as described in [18], as well as in SIW and microstrip technology as detailed in [19] and [20] respectively.

D. Fully canonical filter with 4 poles and 4 transmission zeros

The specifications here considered are: the passband spans from 9.955 to 10.06 GHz, RL of 15 dB and TZs placed at 9.876, 10.2, 9.83 and 10.12 GHz. Like the previous examples there are many synthesizable circuits for these specifications. For example, four cascaded singlets or cascaded singlet-doublet-singlet. However, for this case we consider a circuit of two doublets in cascade as shown in Fig. 17a. Each doublet performs 2 TZs, in the same order of the specifications. They were implemented by using the TM dual-mode cavity described in [21] as shown in Fig. 17b. The unitary inverter that interconnects the doublets was implemented with a waveguide section. The input and output are WR90 sections. The same physical sizing procedure from the previous example was applied here. All dimensions of the filter are written in the caption of Fig. 17. The scattering parameters of the synthesized circuit (solid line) and of the physical filter (dotted line) are illustrated in Fig. 17c.

Note that there are other implementations of doublets in waveguide technology like the generalized TM dual-mode cavity described in [22] or the stubbed oversized TE cavity detailed in [23]. Implementations of doublets in SIW and microstrip technology are addressed in [19] and [24] respectively.

E. Filter with 5 poles and 2 transmission zeros

For this last example consider a filter with: 10 GHz of central frequency F_c, 1% of fractional bandwidth FBW, RL of 18 dB and TZs placed at 10.1515, ∞, ∞, ∞ and 10.2565 GHz. The chosen synthesized topology is cascaded singlet - 3 resonators - singlet as shown in Fig. 18a. Unlike the previous examples, here inverters are implemented with inductive irises and the resonators as 180° transmission lines with unitary impedance. Note that for this approximation to be valid, the impedance Z of the transmission lines have to be:

$$Z = \frac{\pi}{2}\sqrt{\frac{L}{C}}, \tag{16}$$

where L is the inductance and C the capacitance of the resonators. Then, in order to force Z to be unitary, the three central resonant nodes (capacitance and susceptance) are scaled with:

$$\alpha = \frac{\pi}{2}\,\mathrm{FBW}, \tag{17}$$

while adjacent inverters with $\sqrt{\alpha}$. The reference frequency for the 180° electrical length is [17]:

$$F_r = \frac{F_c}{2}\left(-B\sqrt{\frac{L}{C}} + \sqrt{B^2\frac{L}{C} + 4}\right), \tag{18}$$

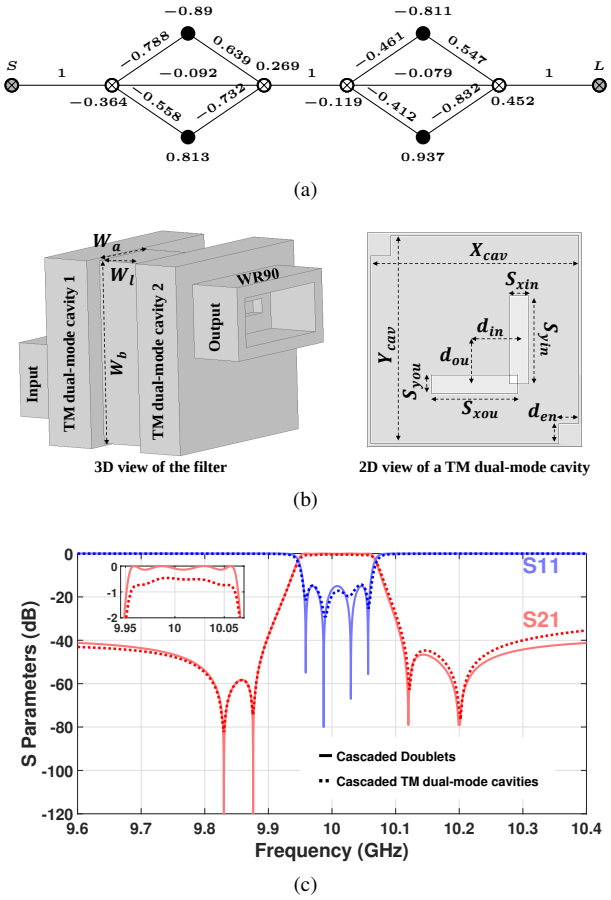

Fig. 17. 4-poles 4-TZ filter. (a) Synthesized Circuit: 2 cascaded doublets connected through a unitary inverter. Black circles are denormalized RNs. Silver crossed circles are unitary source or load. White crossed circles are NRNs. (b) Physical Filter: 2 cascaded TM dual-mode cavities connected through a waveguide section. Dimensions in mm of X_{cav}, Y_{cav}, Z_{cav}, d_{en}, S_{xin}, S_{yin}, S_{xou}, S_{you}, S_z, d_{in}, d_{ou} are respectively for Cavity 1: 33.6, 33.5695, 5.5, 3.2385, 3.0751, 14.264, 13.941, 2.982, 2, 7.2076, and 7.2076; for Cavity 2: 33.848, 33.8095, 5, 3.303, 3.04634, 17.1698, 17.077, 2.9775, 2, 7.5499, and 7.4699. Dimensions in mm of W_a, W_b and W_L are 10.8112, 32.5631 and 5.458 respectively. (c) Scattering parameters of (a) in solid line and (b) in dotted line.

where B is the frequency-independent susceptance of the resonant node (numbers that label the black circles in the figures). The output circuit after scaling and converting the resonators to transmission lines is shown in Fig. 18b.

It is important to note that this last conversion is an approximation, which works well for relatively narrow-band filters and provides preliminary filter dimensions. The physical filter that implements this circuit is shown in Fig. 18c.

Note that the approach we follow in the previous examples for physical dimensioning of the filter is to optimize separately each physical block to behave as closely as possible to the corresponding circuit block, and then put them all together [6] connected through waveguide sections. In this example, since the connections between blocks include irises, we follow the segmentation technique described in [25] and [26]. This technique begins by optimizing the first physical block (connected to source) to behave like the corresponding circuital block, then adding one block at a time and optimizing them so that the frequency response is equivalent to the corresponding

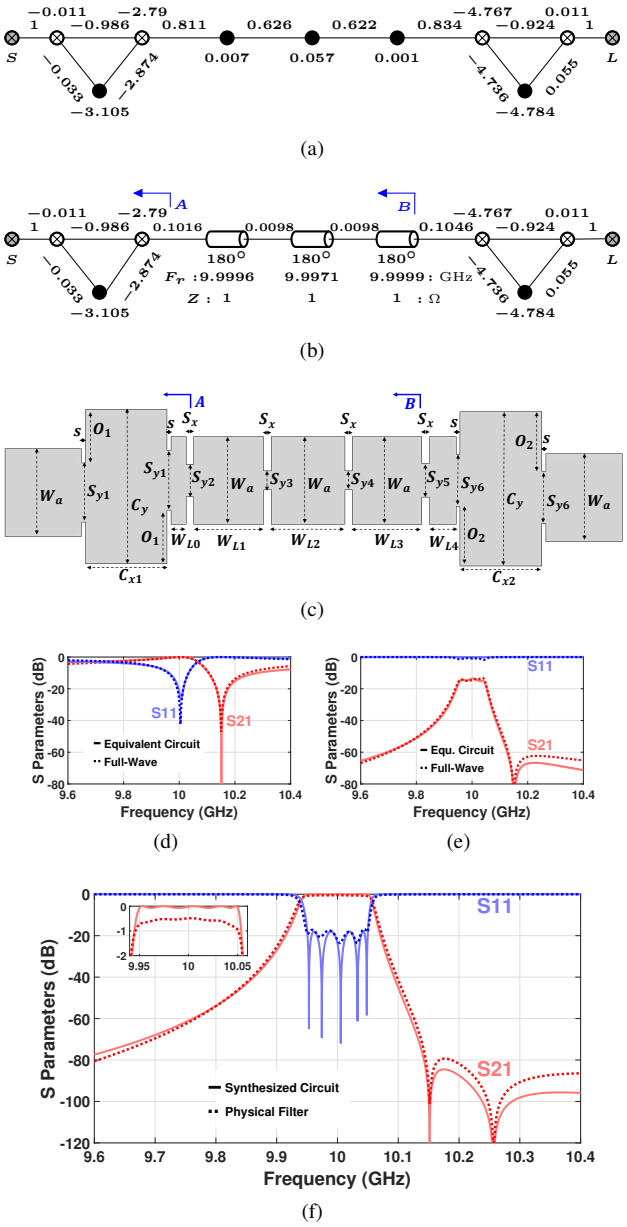

Fig. 18. 5-poles 2-TZ filter. (a) Synthesized Circuit: cascaded singlet - 3 RNs - singlet. Black circles are RNs denormalized with C=$1/(2\pi\, BW)$, L=$1/(C*(2\,\pi\, F_c)^2)$. Silver crossed circles are unitary source or load. White crossed circles are NRNs. (b) Circuit after scaling and converting RNs into transmission lines. (c) Physical filter. Dimensions in mm of W_a, h, $O1$, C_y and O_2 are 22.86, 10.16, 13.971, 40.206 and 15.561 respectively. Dimensions in mm of s, S_x, S_{y1}, S_{y2}, S_{y3}, S_{y4}, S_{y5} and S_{y6} are 1, 2, 15.434, 8.43, 4.912, 4.917, 8.749 and 13.544 respectively. Dimensions in mm of C_{x1}, W_{L0}, W_{L1}, W_{L2}, W_{L3}, W_{L4} and C_{x2} are 21.349, 3.992, 18.282, 19.171, 18.123, 7.015 and 21.412 respectively. (d-e) Scattering parameters from source up to reference section A and B respectively. (f) S-parameters form source to load of (b) in solid line and (c) in dotted line.

circuital part. This must be done until reach the load. To outline the procedure, Fig. 18c shows the response (circuital domain and full wave) of the first circuit block highlighted with the reference section A in Figs. 18b-c. The response of the circuits from the source up to the reference section B is shown in Fig. 18d. Finally, the scattering parameter response from source to load of both circuit and physical filter are illustrated in Fig. 18f.

F. Discussion

Despite the main contribution of this paper is the analytical, novel and flexible synthesis method for cascaded n-tuplets including non-resonating nodes and extracted pole blocks, we have also included within the examples a short review of different physical filter dimensioning techniques, providing some guidelines for the filter implementation in waveguide technology. Note that, despite these practical examples were focused on this technology, the novel synthesis method is not limited to it and the synthesized circuits can be implemented in other technologies. Some references were given for implementations of doublets and singlets in SIW and microstrip technologies. These examples were also focused on filters that include singlets, doublets, and extracted-pole sections. The main reason is that these blocks allow to design even fully canonical and therefore highly selective filters. However, the novel method allows to synthesize filters that include any n-tuplet block, e.g. sextuplets as it was shown in the synthesized filter of Fig 13c.

In addition, one of the theoretical examples also addressed the implementation of complex conjugated TZs for group delay equalization using a quadruplet. This block which was cascaded with singlets, doublets and extracted-poles blocks (Figs. 11 and 12). Although the initial circuit had complex elements in the extracted-pole section that implemented the complex conjugated TZs, the final quadruplet prototype had only real elements (a passive and lossless network). This is consistent with the work in [5], where the quadruplet is synthesized by joining two triplets, which form a fully crossed block (with complex values) like the quadruplet of Fig. 11c, then a completely real coupling matrix is obtained by eliminating one of the cross-couplings, analogous to our procedure. This is also consistent with the section extraction technique, where starting from a lossless transfer function, complex conjugated TZs can be extracted in a quadruplet using lossless components.

It is remarkable, that the novel method allows to synthesize a large set of equivalent circuits that meet the same required electrical performance. However, it is important to clarify that not all circuits are guaranteed to be feasible in all technologies. It is up to the designer to choose the topology or circuit that best suits the target technology. It is also important to mention that it is possible to take advantage of the degrees of freedom available in synthesized circuits to adjust them to particular physical requirements. For example: the three RNs in the middle of the circuit in Fig. 18a were scaled with (17) to be equivalent (roughly) to a 180° transmission line with unity impedance. This was a physical constrain for these resonators to have the same width W_a of the input and output waveguide. Note also that the circuit of Fig. 18b may not be feasible in certain technologies because some coupling values are high in the singlets, however the NRNs with values -2.79 and -4.767 could be scaled by 0.01 (adjacent inverters by 0.1), for example, to get smaller couplings that may be realizable.

Another example on physical constraints is shown in Fig. 15, where in order to avoid NRNs on the extracted-pole blocks (generally implemented as detuned cavities), the circuit was

synthesized and then the NRNs scaled in such a way that after converting the inverters into phased shifters and two shunt susceptances, the NRNs are removed.

Finally, note the relatively low fractional bandwidth of the physical filter examples, limited to a few percent mainly by the frequency dispersion of the waveguide sections. However, it is important to clarify that, since the synthesis method is independent of technology, it is also independent on the bandwidth assigned to the de-normalized filter. Of course, at the time of physical implementation each technology (waveguide, SIW, microstrip) has its own limitations regarding bandwidth.

V. Conclusion

This paper presents a unified analytical method for the synthesis of cascaded n-tuplets prototype filters including non-resonating nodes and extracted pole blocks. This method helps to overcome the issues of accuracy, computation time and uncertainty of optimization methods used to synthesize some topologies, particularly those that include singlets, doublets or mixed topologies. Moreover, the method overcomes the ad-hoc techniques currently used to synthesize specific cascaded n-tuplets by providing a generic procedure independent from n. This new synthesis method is flexible in terms of topologies, allowing freedom in the choice of topologies for a given set of specifications while not changing the synthesis procedure. In addition, the method allows mixed topologies by including extracted-pole blocks in the synthesized circuit if necessary. Several examples are reported to validate the procedure, some of them including the physical sizing procedure starting from the synthesized circuits. Furthermore, the novel filter transformation presented here (from extracted-pole to cross-coupled topology) provides an additional tool available for filter design. Two methods were presented for this purpose, the second being easy to implement since it is based exclusively on matrix operations.

References

[1] N. Yildirim, O. A. Sen, Y. Sen, M. Karaaslan, and D. Pelz, "A revision of cascade synthesis theory covering cross-coupled filters," *IEEE Trans. Microw. Theory Techn.*, vol. 50, no. 6, pp. 1536–1543, Jun. 2002.

[2] A. Garcia-Lamperez, S. Llorente-Romano, and M. Salazar-Palma, "Analytical coupled-resonator filter synthesis method by extraction of fully canonical second order blocks," *IEEE Microw. Wireless Compon. Lett.*, vol. 23, no. 3, pp. 137–139, Mar. 2013.

[3] R. Levy, "Direct synthesis of cascaded quadruplet (cq) filters," *IEEE Trans. Microw. Theory Techn.*, vol. 43, no. 12, pp. 2940–2945, Dec. 1995.

[4] T. Reeves and N. van Stigt, "A method for the direct synthesis of cascaded quintuplets," in *IEEE MTT-S Int. Microw. Symp. Dig.*, vol. 3, Jun. 2002, pp. 1441–1444 vol.3.

[5] S. Tamiazzo and G. Macchiarella, "An analytical technique for the synthesis of cascaded n-tuplets cross-coupled resonators microwave filters using matrix rotations," *IEEE Trans. Microw. Theory Techn.*, vol. 53, no. 5, pp. 1693–1698, May. 2005.

[6] G. Macchiarella, G. G. Gentili, C. Tomassoni, S. Bastioli, and R. V. Snyder, "Design of waveguide filters with cascaded singlets through a synthesis-based approach," *IEEE Trans. Microw. Theory Techn.*, vol. 68, no. 6, pp. 2308–2319, Jun. 2020.

[7] S. Caicedo Mejillones, M. Oldoni, S. Moscato, and G. Macchiarella, "Analytical synthesis of fully canonical cascaded-doublet prototype filters," *IEEE Microw. Wireless Compon. Lett.*, vol. 30, no. 11, pp. 1017–1020, Nov. 2020.

[8] G. Macchiarella, M. Oldoni, and S. Tamiazzo, "Narrowband microwave filters with mixed topology," *IEEE Trans. Microw. Theory Techn.*, vol. 60, no. 12, pp. 3980–3987, Dec. 2012.

[9] Y. He, G. Wang, X. Song, and L. Sun, "A coupling matrix and admittance function synthesis for mixed topology filters," *IEEE Trans. Microw. Theory Techn.*, vol. 64, no. 12, pp. 4444–4454, Dec. 2016.

[10] S. Amari, "Direct synthesis of cascaded singlets and triplets by non-resonating node suppression," in *IEEE MTT-S Int. Microw. Symp. Dig.*, Jun. 2006, pp. 123–126.

[11] U. Rosenberg, J. Ebinger, and S. Amari, "Advanced receive/transmit diplexer design for emerging mm-wave access radio applications," in *IEEE MTT-S Int. Microw. Symp. Dig.*, Jun. 2006, pp. 1217–1220.

[12] S. Amari and G. Macchiarella, "Synthesis of inline filters with arbitrarily placed attenuation poles by using nonresonating nodes," *IEEE Trans. Microw. Theory Techn.*, vol. 53, no. 10, pp. 3075–3081, Oct. 2005.

[13] S. Caicedo Mejillones, M. Oldoni, S. Moscato, G. Macchiarella, M. D'Amico, and G. G. Gentili, "Accurate synthesis of extracted-pole filters by topology transformations," *IEEE Microw. Wireless Compon. Lett.*, vol. 31, no. 1, pp. 13–16, Jan. 2021.

[14] S. Bedrosian, "Converse of the star-mesh transformation," *IRE Trans. Circuit Theory*, vol. 8, no. 4, pp. 491–493, Dec. 1961.

[15] M. van Lier and R. Otten, "Planarization by transformation," *IEEE Trans. Circuit Theory*, vol. 20, no. 2, pp. 169–171, Mar. 1973.

[16] R. J. Cameron, "General coupling matrix synthesis methods for chebyshev filtering functions," *IEEE Trans. Microw. Theory Techn.*, vol. 47, no. 4, pp. 433–442, Apr. 1999.

[17] M. Oldoni, G. Macchiarella, and F. Seyfert, *Synthesis and Modelling Techniques for Microwave Filters and Diplexers: Advances in Analytical Methods with Applications to Design and Tuning*, Feb. 2014.

[18] S. Bastioli, "Nonresonating mode waveguide filters," *IEEE Microwave Magazine*, vol. 12, no. 6, pp. 77–86, Oct. 2011.

[19] S. Sirci, M. . Sánchez-Soriano, J. D. Martínez, and V. E. Boria, "Advanced filtering solutions in coaxial siw technology based on singlets, cascaded singlets, and doublets," *IEEE Access*, vol. 7, pp. 29 901–29 915, 2019.

[20] M. Martinez-Mendoza, D. Canete-Rebenaque, F. J. Perez-Soler, and A. Alvarez-Melcon, "Novel broadside trisection filters employing non-resonating nodes," in *2008 38th Eur. Microw. Conf. (EuMC)*, Oct. 2008, pp. 634–637.

[21] S. Bastioli, C. Tomassoni, and R. Sorrentino, "A new class of waveguide dual-mode filters using tm and nonresonating modes," *IEEE Trans. Microw. Theory Techn.*, vol. 58, no. 12, pp. 3909–3917, Dec. 2010.

[22] C. Tomassoni, S. Bastioli, and R. Sorrentino, "Generalized tm dual-mode cavity filters," *IEEE Trans. Microw. Theory Techn.*, vol. 59, no. 12, pp. 3338–3346, Dec. 2011.

[23] S. Bastioli and R. V. Snyder, "Stubbed waveguide cavity filters," *IEEE Trans. Microw. Theory Techn.*, vol. 67, no. 12, pp. 5049–5060, Dec. 2019.

[24] W. Tang and J. Hong, "Quasi-elliptic function doublet filters without cross coupling," in *2009 Eur. Microw. Conf. (EuMC)*, Oct. 2009, pp. 452–455.

[25] M. Guglielmi, "Simple cad procedure for microwave filters and multiplexers," *IEEE Trans. Microw. Theory Techn.*, vol. 42, no. 7, pp. 1347–1352, Jul. 1994.

[26] D. Martínez Martínez, "Band-pass waveguide filters and multiplexers design by the structure segmentation technique," Bachelor's Thesis, Escuela Técnica Superior de Ingeniería de Telecomunicación, Universidad Politécnica de Cartagena, Jul. 2014.

Steven Caicedo Mejillones was born in Guayaquil, Ecuador, in 1991. He received his Diploma in Telematics Engineering in 2014 and his Master's Degree in Telecommunications in 2017, both from the Escuela Superior Politécnica del Litoral (ESPOL), Guayaquil, Ecuador. From 2014 to 2018, he worked as a planning and optimization engineer for radio access networks in different telecommunications companies in Ecuador, like the mobile operator Claro from América Móvil Group, and since August 2018, he has been an EarlyStage Researcher at SIAE MICROELETTRONICA in Milan, Italy, within the Marie-Curie ITN 5G STEP FWD program framework. Since November 2018, he also has been a Ph.D. candidate at the Politecnico di Milano. His research interests include synthesis and design techniques for microwave filters, filtering antennas and phased array antennas.

Matteo Oldoni was born in Milan, Italy, in 1984. He received the M.Sc. degree in telecommunications engineering, and Ph.D. degree from the Politecnico di Milano, Milan, Italy, in 2009 and 2013, respectively. He is currently with SIAE MICROELETTRONICA in the field of microwave components. His research interests include synthesis and design techniques for microwave filters, algorithms development for computer-aided tuning, and antenna design. Mr. Oldoni was the recipient of the Young Engineers Prize of the 39th European Microwave Conference. Since 2014 he has been part of SIAE R&D Technical Staff.

Stefano Moscato (S'12) received the M.S. and Ph.D. degrees in electronics engineering from the University of Pavia, Pavia, Italy, in 2012 and 2016, respectively. He was with the School of Electrical and Computer Engineering, Georgia Institute of Technology, Atlanta, GA, USA, as a Ph.D. Visiting Student from 2014 to 2015. He is currently with SIAE MICROELETTRONICA. His research activities have focused on the implementation of RF and microwave passive components in substrate-integrated waveguide technology based on standard substrates, ecofriendly materials, and by exploiting the innovative 3-D printing technique. Dr. Moscato was a recipient of an IEEE Microwave Theory and Techniques Society Undergraduate/Pre-Graduate Scholarship in 2012. He was the Chair of the IEEE Student Branch, University of Pavia from 2013 to 2015.
.

Giuseppe Macchiarella (Fellow, IEEE) is currently a Professor of microwave engineering with the Department of Electronic, Information and Bioengineering, Politecnico di Milano, Milan, Italy. His research activity has covered in the past several areas of microwave engineering: microwave acoustics (SAW devices), radio wave propagation, numerical methods for electromagnetic, power amplifiers, and linearization techniques. He has been a Scientific Coordinator of PoliEri, Milan, Italy, a research laboratory on a monolithic microwave integrated circuit (MMIC), which was jointly supported by Politecnico di Milano and Ericsson Lab Italy. He has authored or coauthored more than 150 articles on journals and conferences proceedings. He has been responsible of several contracts and collaborations with various companies operating in the microwave industry. His research activities are mainly focused on the development of new techniques for the synthesis of microwave filters and multiplexers. Prof. Macchiarella has been the Chair of the IEEE Technical Committee MTT-8 (Filters and Passive Components). He has been serving, for several years, on the Technical Program Committee (TPC) of the IEEE International Microwave Symposium and European Microwave Conference.

Michele D'Amico was born in Italy, in 1965. He received the M.S. degree in electronic engineering from Politecnico di Milano, Milan, Italy, in 1990 and the Ph.D. degree in mathematics from the University of Essex, Colchester, U.K., in 1997. From 1993 to 2002, he was an Assistant Professor with the Dipartimento di Elettronica e Informazione (DEI), Politecnico di Milano. He has been a Visiting Researcher with the European Space Agency and with the Rutherford Appleton Laboratory, Chilton, U.K. Since 2002, he has been an Associate Professor of applied electromagnetics with DEI. Since May 2004, he has been responsible for the experimental activities of the Centro Studi Applicazioni Radio Elettriche Laboratory, Politecnico di Milano, Busto Arsizio, Italy, where he is mainly dedicated to electromagnetic compatibility. His research interests include radarmeteorology, electromagnetic wave propagation in the troposphere, and antennas.

Gian Guido Gentili received the Laurea degree in electronics engineering from the Politecnico di Milano, Milan, Italy, in 1987. He was a Visiting Scholar with Politecnica de Madrid, Madrid, Spain, in 1993 and 1995. He joined the Dipartimento di Elettronica ed Informazione, National Research Council (CNR), Center for Space Telecommunications, Politecnico di Milano, in 1989, as a Researcher. In 2001, he became a Senior CNR Researcher. He became an Associate Professor at the Politecnico di Milano in 2002. He is responsible for the Electromagnetics Laboratory, Politecnico di Milano, "Wavelab." His research interests include a numerical method for electromagnetics (finite elements, method of moments, and mode matching), antennas and feed systems for terrestrial and space applications, microwave passive devices and filters, plasmonics, and terahertz radiation.

Goran Biscevic received his Dipl.Ing. degree and the M.Sc. degree in Telecommunications from FER (Faculty of Electrical Engineering and Computing), University of Zagreb, Croatia, in 1987 and 1995, respectively. After a few years with Nikola Tesla (now Ericsson Nikola Tesla) in Zagreb and a Master Course in Information Technology at CEFRIEL (Milan, Italy), in 1991 he joined SIAE MICROELETTRONICA. Since then, he has held various positions in R&D labs, and has gained experience in analog, mixed and digital signal processing, with particular emphasis on digital modem implementation, DSP algorithms, synchronization methods, FEC and coded modulation schemes, digital countermeasures against RF impairments and design on FPGAs. Since 2013 he has been part of SIAE R&D Technical Staff, and his main activity regards innovation topics in wireless transmission systems.